

Simulation of autosoliton optical pulses in high-speed fibreoptic communication systems

A.I. Latkin

Abstract. The propagation of a pulse in a fibreoptic communication link with periodically included regenerators – nonlinear optical loop mirrors, is studied. The autosoliton propagation regime of the optical pulse is revealed. It is shown that the inclusion of a ring mirror to the communication link leads to a substantial increase in the transmission distance of the pulse at a small negative average dispersion in the link.

Keywords: fibreoptic communication links, autosoliton, nonlinear optical loop mirror, optical regeneration.

The transmission of dispersion-controlled pulses is a key problem in the development of high-speed fibreoptic communication links [1]. The optical regeneration of a signal also plays an important role. In this case, the signal transmission rate in communication links is substantially limited by the spontaneous emission noise introduced by amplifiers. Optical regenerators can be used as nonlinear filters suppressing low-power noise and reconstructing the shape of transmitted pulses. Note that the use of electric regenerators severely restricts the signal transmission rate in communication links. Therefore, the development of all-optical regenerators is an urgent problem.

Optical regenerators can be based on fibre interferometers; for example, a nonlinear optical loop mirror (NOLM), which is a fibreoptic analogue of the Sagnac interferometer, can be used. Due to its nonlinear transfer function, a NOLM can reconstruct the signal shape [2]. A substantial increase in the data transmission distance in communication links achieved with the help of NOLMs was first demonstrated in [3, 4].

We simulated a communication link consisting of the equal numbers of sections of a standard single-mode fibre (SMF) and a dispersion-compensating fibre (DCF). The scheme of a fibreoptic communication link is shown in Fig. 1. The experiment on the data transmission through one channel in this communication link at a rate of 40 Gbit s⁻¹ showed that the use of a NOLM in the link

resulted in a significant increase in the data transmission distance [5].

The communication link under study contains alternating SMFs and DCFs. All the SMFs and DCFs are backward pumped by a Raman fibre laser at $\lambda_p = 1455$ nm. This wavelength is lower than the carrier signal wavelength $\lambda_s = 1553$ nm, so that the pump-wave energy is transferred to the signal due to Raman scattering. The length of the first SMF section is 77 km, that of the second one is 88 km, and the lengths of DCF sections are specified by the value of the average dispersion in the link. NOLMs are included into the link at the beginning of each periodic section behind a Gaussian filter with the spectral width $B_{opt} = 160$ GHz. The NOLM consists of a 70:30 optical coupler and a dispersion-shifted fibre (DSF). In front of the NOLM, an erbium-doped fibre amplifier (EDFA) with the gain $G = 23$ dB (preamplifier) is located to amplify a signal up to the power required for the NOLM operation in a nonlinear regime. Behind the NOLM an attenuator with $G = -23$ dB is located to compensate for the excess signal power. At the end of a periodic section, an EDFA with $G \simeq 11$ dB is located.

We assumed that the splice losses between the SMF and DCF sections were -2 dB. We also assume that attenuation losses in the sections of the link are compensated by Raman amplifiers and losses in NOLMs, filters, and splice losses are compensated by EDFAs located at the end of each periodic section.

The aim of the paper is to study numerically the possible propagation regimes of a single pulse in this link and to determine the parameters allowing a significant increase in the data transmission distance in the communication link.

The propagation of a signal in an optical fibre is described by the generalised nonlinear Schrödinger equation [6]

$$i \frac{\partial A}{\partial z} - \frac{\beta_2}{2} \frac{\partial^2 A}{\partial t^2} - i \frac{\beta_3}{6} \frac{\partial^3 A}{\partial t^3} + \gamma |A|^2 A = -i \frac{\alpha}{2} A. \quad (1)$$

Here, A is the envelope of the electric field of the pulse; z is the coordinate along the fibre; t is the ‘delayed’ time related to the physical time t_{phys} by the expression $t = t_{phys} - z/v_g$; v_g is the group velocity of a packet; $\beta_2 = d(1/v_g)/d\lambda$ is the group-velocity dispersion; $\beta_3 = d\beta_2/d\omega$; $\omega = 2\pi c/\lambda$ is the frequency; α is the attenuation coefficient; $\gamma = 2\pi n_2/\lambda A_{eff}$ is the nonlinearity coefficient; A_{eff} is the effective area of a mode; and n_2 is the nonlinear refractive index of the fibre.

Note that Eqn (1) describes only the propagation of a signal in a fibre with the specified coefficients β_2 , β_3 , γ , and

A.I. Latkin Institute of Automation and Electrometry, Siberian Branch, Russian Academy of Sciences, prosp. akad. Koptyuga 1, 630090 Novosibirsk, Russia; e-mail: a.i.latkin@ngs.ru

Received 24 September 2004; revision received 30 November 2004
Kvantovaya Elektronika 35 (3) 273–277 (2005)
Translated by M.N. Sapozhnikov

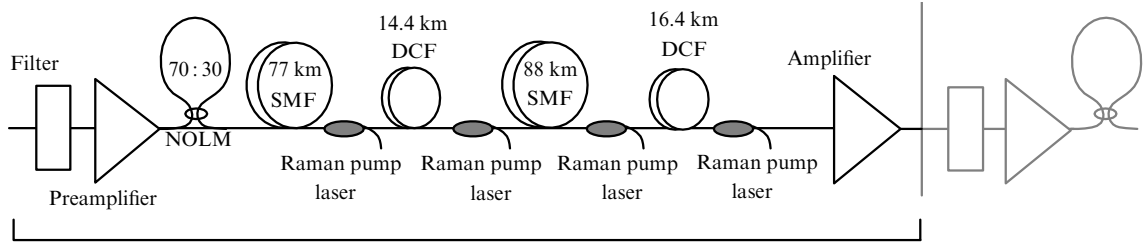


Figure 1. Scheme of the periodic section of the fibreoptic communication link.

α . However, a real communication link contains fibres of two types (SMF and DCF) with different values of these coefficients and also includes filters, amplifiers, and NOLMs. The simulation was performed in the following way: Equation (1) was solved for a link section with a certain set of values of the coefficients; then, the signal propagated through a lumped device was transformed in accordance with the transfer function of this device and its evolution was again described by Eqn (1) (now with different values of β_2 , β_3 , γ , and α), and this procedure was repeated by a required number of times.

The operation principle of an optical filter is based on the multiplication of the distribution of the Fourier transform of the pulse amplitude $A(\omega)$ by the transfer function of the filter. This function has a Gaussian shape with the unit amplitude at the carrier frequency $\omega_0 = 2\pi c/\lambda_s$ and its FWHM is B_{opt} . The action of an optical filter with the transfer function $R(\omega)$ is represented as $A_{\text{out}}(\omega) = A_{\text{in}}(\omega)R(\omega)$.

The amplitude of a signal propagated through an EDFA is multiplied by the gain $G = 10 \lg[G(\text{dB})]$ [6]. A Raman amplifier performs distributed amplification, and when the pump-wave power P_p greatly exceeds the signal power P_s (in our case $P_p \sim 1 \text{ W}$, $P_s \sim 1 \text{ mW}$), we can neglect the effect of the signal on the pump wave and assume that the pump wave exponentially attenuated due to fibre losses, so that $P_p = P_0 \exp[-\alpha_p(L-z)]$, where L is the range between lasers generating the pump wave, and α_p is the attenuation coefficient of the pump wave. As a result, the quantity α in Eqn (1) should be replaced by $\alpha_{\text{eff}} = \alpha - 2g_0 \exp[-\alpha_p(L-z)]$. We also take into account that amplifiers introduce the spontaneous emission noise. The latter noise can be neglected in the problem on propagation of a single pulse, but it should be considered in simulations of data transmission in communication links.

A nonlinear optical ring mirror consists of a fibre loop with a high nonlinearity coefficient and an optical coupler. A signal coupled into such a device is divided in the optical coupler into signals counterpropagating in the ring (the amplitude ratio of the signals is 70:30 and $\pi/2$ is added to the phase of one of the signals). Equation (1) is solved separately for each signal with the corresponding initial conditions and then their interference in the optical coupler is taken into account [2].

Equation (1) was solved numerically by the method of splitting into linear and nonlinear parts. The linear part of the equation was solved by using the fast Fourier transform [7, 8]. The values of β_2 , β_3 , γ , and α for fibres of different types are presented in Table 1.

Consider first the propagation of a single pulse in the communication link. The NOLM parameters are specified so that the output signal power P_{out} would be equal to the

Table 1. Parameters of fibres of different types.

Parameter	SMF	DCF	DSF
α_s at $\lambda_s = 1553 \text{ nm/dB km}^{-1}$	0.2	0.52	0.2
α_p at $\lambda_p = 1455 \text{ nm/dB km}^{-1}$	0.279	0.87	–
$A_{\text{eff}}/\mu\text{m}^2$	80	20	54.1
$\beta_2/\text{ps nm}^{-1} \text{ km}^{-1}$	16.2	–86.9	2.8
$\beta_3/\text{ps nm}^{-2} \text{ km}^{-1}$	0.037	0.058	0.069
$n_2/\text{m}^2 \text{ W}^{-1}$	2.7×10^{-20}	2.7×10^{-20}	2.7×10^{-20}

signal power P_{in} at the mirror input. In this case, a point behind the first maximum of the transfer function is selected [2], so that weak power variations will not cause the unbalance of the mirror, i.e., the positive feedback will exist (Fig. 2), resulting in the self-control of the pulse energy, in other words, in the formation of an autosoliton after the repeated propagation of the pulse through the NOLM. Note that in our calculations, unlike [3, 4], the NOLM fibre has nonzero second- and third-order dispersions. As a result, the amplitude and phase of the output signal depend not only on its initial amplitude (power) but also on the pulse width. Therefore, the formation of a stable autosoliton is complicated. However, if the parameters of the communication link and NOLM are selected properly, the energy of the signal is established already after a few first periodic sections of the communication link.

The initial pulse was taken in the form of a Gaussian with the peak power $P_{\text{peak}} = 12.5 \text{ mW}$ and the FWHM $T_{0.5} = 4.2 \text{ ps}$. Figure 3 shows a sequence of pulses extracted

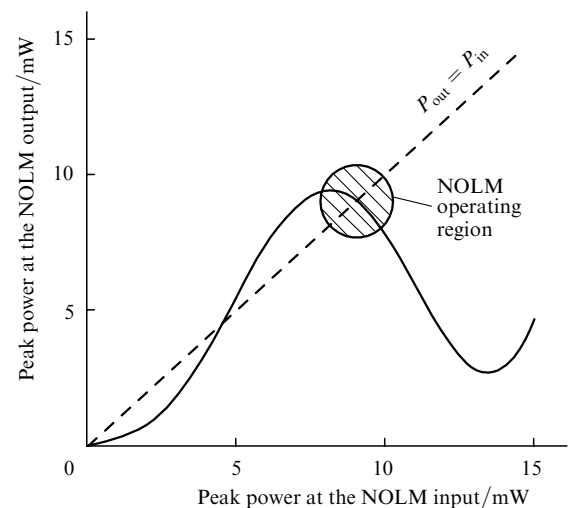


Figure 2. Transfer function of a ring mirror.

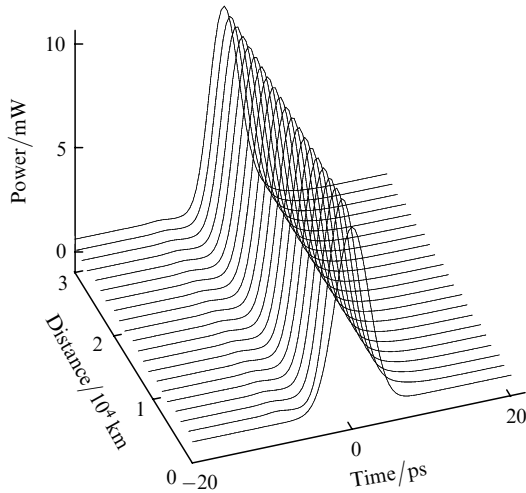


Figure 3. Dynamics of a Gaussian pulse with the FWHM of 4.2 ps and the initial peak power $P_0 = 12.5$ mW at the NOLM input.

at the end of periodic sections, i.e., the so-called slow dynamics of the pulse. Variations in the pulse parameters within one periodic section are called the fast pulse dynamics.

The centre of a pulse propagating in a communication link shifts systematically with time because the mean value of β_3 in the link is nonzero. For this reason, the amplitude distributions $A[z, t - \bar{t}(z)]$ are presented for each value of z in Fig. 3, where

$$\bar{t}(z) = \frac{\int_{-\infty}^{\infty} t |A(z, t)|^2 dt}{\int_{-\infty}^{\infty} |A(z, t)|^2 dt}. \quad (2)$$

The type of pulse propagation is determined by the communication-link parameters, in particular, by the EDFA gain G . By varying the gain, we can obtain a stable autosoliton regime, when the pulse energy at the NOLM input does not change from section to section. Figure 4 shows the dependences of the pulse energy on the propagated distance for several values of G . One can see that a stable propagation of the pulse is possible only in a certain range of G .

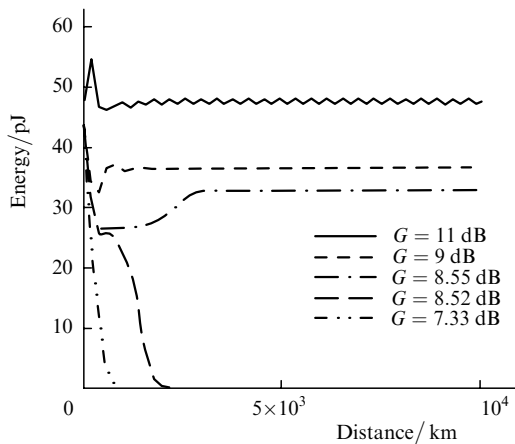


Figure 4. Dependences of the pulse energy on the propagation distance for different values of the gain G .

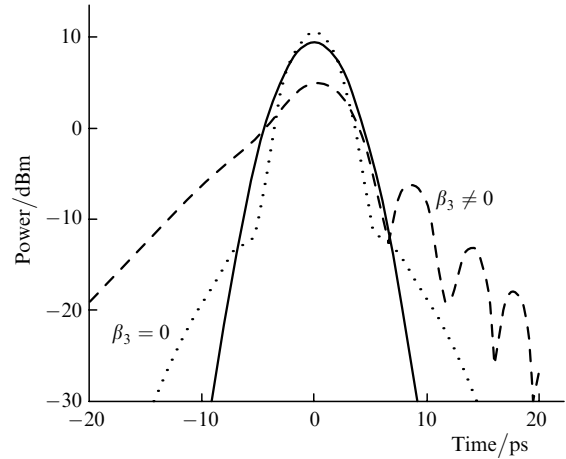


Figure 5. Time dependences of the power of the initial Gaussian pulse (solid curve) and autosolitons in the communication link for $\beta_3 = 0$ (dotted curve) and $\beta_3 \neq 0$ (dashed curve).

Due to the nonzero value of β_3 , the autosoliton has a complex asymmetric shape (the dashed curve in Fig. 5; for clearness, the power is measured in decibels with respect to milliwatt [$P(\text{dBm}) = 10 \lg[P(\text{mW})/1 \text{ mW}]$]). As a result, even when the pulse energy and its rms width, defined as

$$\bar{T} = \left[\frac{\int_{-\infty}^{\infty} t^2 |A(z, t)|^2 dt}{\int_{-\infty}^{\infty} |A(z, t)|^2 dt} \right]^{1/2} \quad (3)$$

are constants, the peak power of the pulse and its FWHM can oscillate periodically in contrast to the link with $\beta_3 = 0$ [3, 4]. For comparison, Fig. 5 shows the pulse shape for a link with the zero mean value of β_3 (dashed curve) and the initial Gaussian pulse (solid curve).

The fast dynamics of the peak pulse power during one section is shown in Fig. 6. The local peaks correspond to the locations of Raman lasers generating the pump wave.

Let us now simulate data transmission in the link. The data were transmitted through one channel at a rate of 40 Gbit s^{-1} . The parameters of the link and NOLM were selected to provide the propagation of an autosoliton in the link (i.e., the model problem of propagation of a single pulse

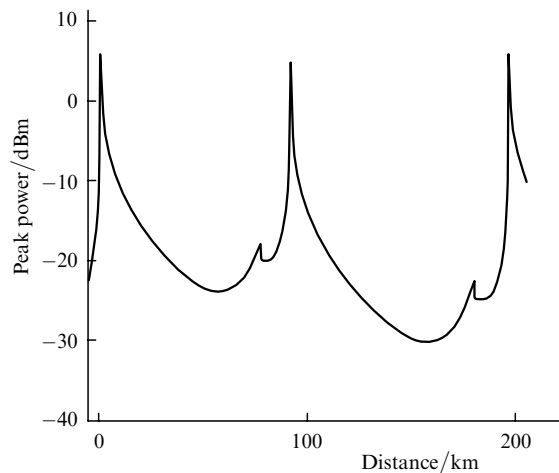


Figure 6. Dependence of the peak power on the propagation distance for one periodic section of the communication link.

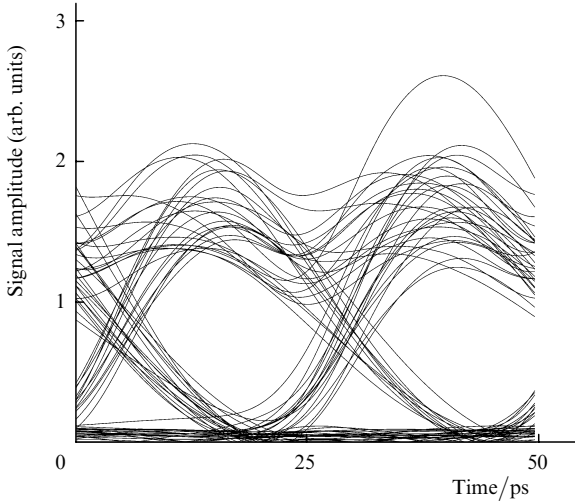


Figure 7. Eye-diagram for the communication link without a regenerator; Q factor is equal to 6 at a distance of 1600 km (maximal Q for a periodic section).

in a communication link can be considered as a preliminary optimisation of the communication-link parameters to increase its transmission capacity). The main characteristic of the link is the data transmission distance, i.e., the maximum distance at which the bit error rate (BER) does not exceed the critical value 10^{-9} for a given transmission rate. The simulation of data transmission took into account the spontaneous emission noise because it is one of the main factors restricting the transmission distance in the link.

Instead of the BER, the so-called Q factor is often used, which is related to the BER by the expression

$$\text{BER} = \frac{1}{2} \operatorname{erfc} \left(\frac{Q}{\sqrt{2}} \right) \approx \frac{\exp(-Q^2/4)}{\sqrt{2\pi}Q}. \quad (4)$$

The value $Q = 6$ corresponds to the $\text{BER} = 10^{-9}$.

We varied the main parameters affecting the transmission distance – the average dispersion D_{av} in the link

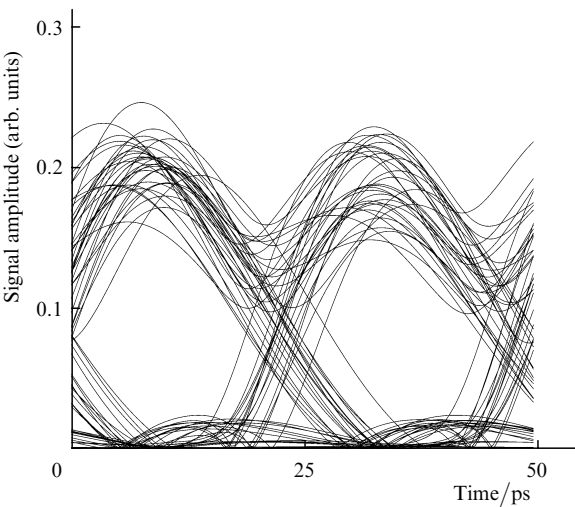


Figure 8. Eye-diagram for the communication link with a regenerator; Q factor is equal to 9 at a distance of 7000 km (maximal Q for a periodic section).

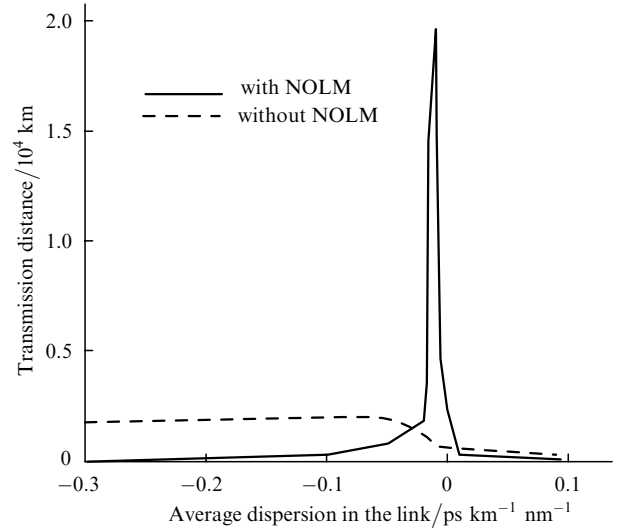


Figure 9. Dependences of the transmission distance on the average dispersion in the communication link with and without a regenerator.

and the peak power P_{peak} of transmitted pulses in order to determine the maximum possible transmission distance.

The transmitted data were simulated by a pseudorandom sequence of length $2^7 - 1$ bit. For each set of parameters, the calculations were performed with seven independent bit sequences and then the median value of the transmission distance was found [9]. Figures 7 and 8 show the so-called eye-diagrams for a link without a NOLM (Fig. 7) and a link containing a NOLM (Fig. 8). The distributions of pulse amplitudes in each pair of successive bit intervals (of length $T_b = 25$ ps for the 40-Gbit s^{-1} rate) in these diagrams are shifted in time, so that all of them are superimposed in the interval from 0 to 50 ps. The eye-diagrams clearly show that the sequence of pulses in the link without a NOLM is distorted much stronger already at a distance of 1600 km compared to the link with a NOLM at a distance of 7000 km.

Figure 9 shows the dependence of the transmission distance on the average dispersion for the link containing a NOLM (solid curve) and without a NOLM (dashed curve). This dependence for the link with the NOLM has a sharp maximum corresponding to the transmission distance equal to 20000 km when the average dispersion is $D_{\text{av}} = -0.01$ $\text{ps km}^{-1} \text{nm}^{-1}$, whereas the dependence for the link without the NOLM is smooth and the transmission distance does not exceed 2000 km. For comparison, the transmission distance in the link with a NOLM obtained in experiment [5] was increased to 4000 km. The dependence of the transmission distance on the input peak pulse power is very weak in a rather broad power range from 7 to 18 mW.

Thus, we have demonstrated the possibility to increase the data transmission distance in communication links by using the following algorithm. First the model problem is solved, the NOLM and link parameters (the gain G) being selected to provide the existence of autosoliton solutions. Then, data transmission is directly simulated by varying the main parameters affecting the transmission distance: the average dispersion in the link and the peak power of transmitted pulses.

The numerical simulation of the communication link containing NOLM regenerators has shown that autosolitons, i.e., pulses with periodically recovered parameters can

propagate in this link. Due to the nonzero third-order average dispersion in the link, the autosoliton has a complex shape, so that it is reasonable to characterise such a pulse not by its peak power and FWHM but by the total energy and rms width. The communication link with one frequency channel and the 40-Gbit s⁻¹ transmission rate has been optimised. The transmission distance in the communication link containing a NOLM achieves 20000 km, exceeding by an order of magnitude that for the link without a NOLM.

References

- [doi](#) 1. Alleston S.B., Harper P., Penketh I.S., Bennion I., Doran N.J., Ellis A.D. *Electron. Lett.*, **35** (10), 823 (1999).
- Agrawal G.P. *Applications of Nonlinear Fiber Optics* (New York: Academic Press, 2001).
- Boscolo S., Turitsyn S.K., Blow K.J. *Techn. Dig. Nonlinear Guided Waves Their Applications (NLGW 2001)* (Clearwater, Florida, USA, 2001) p.248, MC71.
- Boscolo S., Turitsyn S.K., Blow K.J. *Techn. Dig. Opt. Fiber Commun. Conf. (OFC 2001)* (Anaheim, California, USA, 2001) MF6.
- [doi](#) 5. Gray A., Huang Z., Lee Y.W.A., Klurshichev I.Y., Bennion I. *Opt. Lett.*, **29** (9), 926 (2004).
- Agrawal G.P. *Fiber-Optic Communication Systems* (New York: John Wiley & Sons, Inc., 1997).
- Cooley J.W., Tukey J.W. *Math. Comput.*, **19**, 297 (1965).
- Agrawal G.P. *Nonlinear Fiber Optics* (New York: Academic Press, 2001).
- [doi](#) 9. Shapiro E.G., Fedoruk M.P., Turitsyn S.K. *Electron. Lett.*, **37** (19), 1179 (2001).